JOURNAL OF MATERIALS SCIENCE 22 (1987) 1482–1488

Statistical analysis of the effect of surface grinding on the strength of alumina using Weibull's multi-modal function

Y. MATSUO, T. OGASAWARA, S. KIMURA
Department of Inorganic Materials, Faculty of Engineering, Tokyo Institute of Technology, 2-12-1, Ookayama, Meguro-ku, Tokyo 152, Japan

E. YASUDA
Research Laboratory of Engineering Materials, Tokyo Institute of Technology, 4259 Nagatsuta-cho, Midori-ku, Yokohama 227, Japan

Statistical analysis of the effect of surface grinding on the fracture strength of ceramics was performed and a new distribution function based on multi-modal Weibull distribution function has been suggested. The experimental verifications were carried out on alumina specimens ground in various directions using diamond wheels which have different abrasive diameters. The theory agreed well with the experimental results.

1. Introduction

When ceramic materials are used as structural components, it is necessary to machine them adequately after sintering. Grinding with diamond wheels is commonly used for machining the structural ceramics because of the advantages of the costs and accuracy. However, during grinding, it is well known that the surface of the ceramics may be deformed plastically and scratch cracks such as median/radial and lateral cracks may be induced by the effects of the residual stresses at the elastic–plastic boundary along the grinding groove [1–6]. The mechanical properties of ceramic materials are significantly influenced by these machining-induced cracks, which has been reported frequently. For example, the effect of grinding forces during grinding and grinding parameters such as the depth of cut, the abrasive particle diameters, the wheel speed, and the workpiece velocity have been studied [7–11]. The effect of microstructures, residual stresses and grinding direction on grinding treatment of the ceramics have also been investigated. Mecholsky *et al.* [12], Andersson *et al.* [13] and Rice *et al.* [4] have found that the bending strength parallel to the grinding direction is greater in magnitude than that perpendicular to the grinding direction. The effect of surface finish on the strength–grain size relation has been investigated by Tressler *et al.* [14], Cranmer *et al.* [15], and Rice [4]. It was found from these works that the strength of the ceramics with fine grain size is significantly influenced by the machining-induced cracks. Residual stresses induced by grinding may have a strong influence on the mechanical properties of materials. Kirchner *et al.* [5] and Hakulinen [16] have discussed this problem to some extent. Mixed-mode fractures under the multi-axial stress states have been investigated by Petrovic *et al.* [17], Freiman *et al.* [18] and Marshall [19]. Marshall, in particular, discussed the anisotropy of the strengths of brittle materials with a ground surface, but did not consider the strength distributions of brittle materials. Despite many investigations of these problems, the statistical analysis of the effect of surface grinding on the strength of ceramic materials has been little reported.

When the fracture strength of ceramics is analysed, a statistical analysis based on fracture mechanics is necessary. The statistical approaches based on the weakest link theory have been studied for brittle fracture under multi-axial stress states by Weibull [20], Batdorf and Crose [21, 22], Evans [23, 24] and Matsuo [25, 26]. On the other hand, Bolotin [27], Matsuo [25], and Johnson [28] carried out a statistical analysis based on the multi-modal Weibull distribution function for brittle materials having many kinds of fracture origin.

In this work, based on the multi-modal Weibull distribution function under multi-axial stress state [25, 26], we formulate the distribution function of the fracture strength of a body which has surfaces machined by a grinding process. Experimental verifications are performed on alumina specimens which are ground in various directions using diamond wheels of different abrasive diameters.

2. Theoretical analysis

A scratch cracks system model induced by the grinding of ceramics was suggested by Richerson [6] as shown in Fig. 1a. The scratch cracks system consists of the median crack (longitudinal), the lateral crack and the radial crack (transverse). We assume that only the median-type crack beneath the grinding groove can affect the strength of alumina ceramics used in our experiments because, as seen in Section 4, the strengths of specimens ground parallel to their axis is not affected by the abrasive diameter of the grinding

0022–2461/87 $03.00 + .12

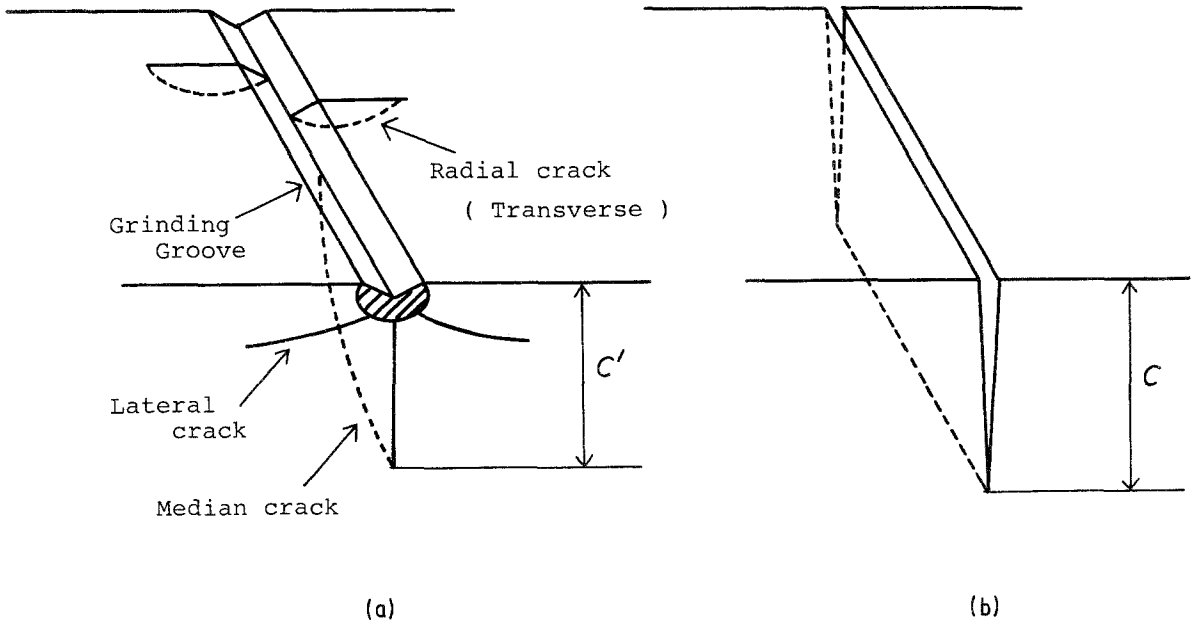

Figure 1 Schematic drawing of the scratch cracks caused by grinding: (a) scratch-cracks systems after Richerson [6]; (b) equivalent part-through edge crack.

wheel. In general, the median-type cracks seem to be flat semi-elliptical cracks. However, the stress intensity factors (K_{II} and K_{III}) for these cracks have not yet been calculated analytically as far as we know. Therefore, we assume that a flat semi-elliptical crack is equivalent to a part-through edge crack shown in Fig. 1b, i.e. we consider a one-to-one correspondence between the crack depth C' and C in these figures and we do not take into consideration the effects of the residual stress and stress concentration of the grinding groove explicitly. Since the crack depths C' and C are sufficiently small compared with that of the specimen, the stress states of an edge crack lying on a tensile-stressed surface of a specimen subjected to a bending moment can be expressed as shown in Fig. 2a, where σ and τ are the normal stress and the shear stress, respectively, δ is the mean interval of the grinding grooves (see Fig. 2b).

2.1. General formula for arbitrary stress state

The multi-modal Weibull distribution function, expressed by Equation 1, is that most suitable for describing the fracture phenomena of brittle materials which involve many kinds of fracture origin

$$F(\sigma) = 1 - \exp\left\{-\sum_{i=1}^{K} Bi\right\} \quad (1)$$

where $F(\sigma)$ is the fracture probability of the material under consideration, k is the number of types of fracture origin and Bi is the risk of rupture caused by the ith fracture origin.

Let us assume that there are numerous intrinsic cracks in a body and median cracks on the ground surfaces of a body. First, we consider the intrinsic cracks, i.e. internal cracks ($i = 1$), isotropically distributed surface cracks ($i = 2$), and edge cracks ($i = 3$). Isotropic surface cracks are also supposed to be equivalent to part-through edge cracks shown in Fig. 1b and the edge cracks to be fan-shaped, perpendicular to an edge of a body. For an arbitrary stress state, the risks of rupture, B_1, B_2 and B_3, are given respectively, by the following equations, by using the multiaxial distribution function for fracture [26]:

$$B_1 = (2/\pi)\int_V \int_0^{\pi/2}\int_0^{\pi/2} [(Z_1 - \sigma_{u1})/\sigma_{01}]^{m_1} \times Y(Z_1, \sigma_{u1}) \sin\psi_1 \, d\psi_1 \, d\psi_2 \, dV \quad (2)$$

$$B_2 = (2/\pi)\int_A \int_0^{\pi/2} [(Z_2 - \sigma_{u2})/\sigma_{02}]^{m_2} \times Y(Z_2, \sigma_{u2}) \, d\psi_2 \, dA \quad (3)$$

$$B_3 = \int_L [(Z_3 - \sigma_{u3})/\sigma_{03}]^{m_3} Y(Z_3, \sigma_{u3}) \, dL \quad (4)$$

where ψ_1 and ψ_2 are the polar co-ordinates; dV, dA and dL are the volume element, surface element and line element, respectively; m_i, σ_{0i} and σ_{ui} are Weibull's parameters and $Y(\ )$ is a step function.

For median-type scratch cracks ($i = 4$) induced by the grinding process, the risk of rupture B_4 can easily be expressed as

$$B_4 = \int_L \{(Z_4 - \sigma_{u4})/\sigma_{04}\}^{m_4} Y(Z_4, \sigma_{u4}) \, dL \quad (5)$$

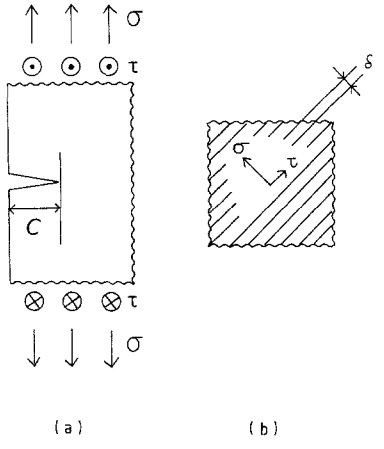

Figure 2 The stress state of the equivalent part-through edge crack: (a) stress systems; (b) grinding groove direction.

where dL is a line element along a grinding groove. Suppose that there is a sufficient number of grinding grooves within an arbitrary small surface element, dA, on a ground surface. Because dL can be expressed by $dL = dA/\delta$, we finally obtain the next useful equation:

$$B_4 = \frac{1}{\delta}\int_A \{(Z_4 - \sigma_{u4})/\sigma_{04}\}^{m_4} Y(Z_4, \sigma_{u4})\, dA \quad (5)'$$

2.2. Analysis of four-point bending test

We now analyse the fracture probability distribution function of a rectangular cross-sectioned brittle specimen subjected to four-point bending load. The coordinate systems used in the analysis are shown in Fig. 3. In the following analysis we suppose that:

1. fracture only occurs at the bottom surface and the edges in tensile-stressed regions ($B_1 = 0$);
2. there are two types of surface cracks which cause fracture, namely, the isotropically distributed surface cracks ($i = 2$) and the median-type scratch cracks ($i = 3$);
3. all location parameters are zero.

We use the next experimental relation as an unstable crack extension condition for mixed modes, which corresponds to the so-called G_c criterion.

$$K_I^2 + K_{II}^2 + (E'/E)(1 + \nu)K_{III}^2 = K_{Ic}^2,$$
$$E' = E/(1 - \nu^2) \quad (6)$$

where E and ν are Young's modulus and Poisson's ratio, respectively and K_{Ic} is the fracture toughness for Mode I cracks. Because the equivalent normal stress Z_i is defined as [25, 26] $Z_i = K_{Ic}/Y(\pi C)^{1/2}$ where Y is the shape factor and C the crack size, we obtain Z_2, Z_3 and Z_4 as

$$Z_2 = [\sigma^2 + \tau^2/(1 - \nu)\beta^2]^{1/2} \quad (7)$$
$$Z_3 = \sigma \quad (8)$$
$$Z_4 = \{\sigma^2 + \tau^2/(1 - \nu)\beta^2\}^{1/2} \quad (9)$$

where σ and τ are given as functions of two principal stresses σ_1 and σ_2 as

$$\begin{pmatrix}\sigma\\ \tau\end{pmatrix} = \begin{pmatrix}\cos^2\theta & \sin^2\theta\\ -\sin\theta\cos\theta & \sin\theta\cos\theta\end{pmatrix}\begin{pmatrix}\sigma_1\\ \sigma_2\end{pmatrix} \quad (10)$$

Substituting $\sigma_1 = \sigma_f = 3WL_1/4bh^2$ ($L_1 < x < L_1 + L_2$) and $\sigma_2 = 0$ into Equations 7 to 9 we obtain

$$Z_2 = \sigma_f \cos\theta\,\{\cos^2\theta + \sin^2\theta/(1 - \nu)\beta^2\}^{1/2}, \quad (0 < \theta \leqslant \pi/2) \quad (7)'$$
$$Z_3 = \sigma_f \quad (8)'$$
$$Z_4 = \sigma_f \sin\phi\{\sin^2\phi + \cos^2\phi/(1 - \nu)\beta^2\}^{1/2} \quad (\phi = \text{const.}) \quad (9)'$$

As $\beta = 1.1215$ and $\nu = 0.23$ (for alumina), the term $(1 - \nu)\beta^2$ becomes nearly equal to unity, which leads to the following simple equations:

$$Z_2 = \sigma_f \cos\theta, \quad Z_3 = \sigma_f, \quad Z_4 = \sigma_f \sin\phi$$

Substituting the above equations into Equations 2 to 4, we finally obtain

$$F(\sigma) = 1 - \exp\left\{-\sum_{i=2}^{4} B_i\right\} \quad (12)$$

$$B_2 = (\sigma_f/\sigma_{02})^{m_2}(1/\pi)A_{eo}B[\tfrac{1}{2},(m_2 + 1)/2]$$
where $A_{eo} = b\{2L_1/(m_2 + 1) + L_2\}$ (13)

$$B_3 = (\sigma_f/\sigma_{03})^{m_3}L_{eo}$$
where $L_{eo} = 4L_1/(m_3 + 1) + 2L_2$ (14)

$$B_4 = (\sigma_f/\sigma_{04})^{m_4}(1/\delta)A_{eo}\sin\phi$$
where $A_{eo} = b\{2L_1/(m_4 + 1) + L_2\}$ (15)

2.3. Estimation of Weibull parameters

Equation 12 involves six unknown Weibull parameters which must be estimated from experimental data. In order to obtain accurate estimates, we suggest a new method called the "two-step estimation method".

2.3.1. First step

When $\phi = 0°$, B_4 becomes zero. Therefore, Equation 12 involves four unknown parameters (σ_{02}, m_2, σ_{03}, m_3). If we can separate each experimental data into that caused by surface or edge cracks, then we can easily estimate the parameters using the multi-maximum likelihood method [29–31]. In this case, the maximum likelihood equations are written as

$$\frac{n_i}{m_i} - n_i\frac{\sum_{i=1}^{n}\sigma_i^{m_i}\ln\sigma_i}{\sum_{i=1}^{n}\sigma_i^{m_i}} + \sum_{i=1}^{n_i}\ln\sigma_i = 0$$
$$\sigma_{0i} = \left\{(A_{eo}/n_i)\sum_{i=1}^{n}\sigma_i^{m_i}\right\}^{1/m_i} \quad (16)$$

2.3.2. Second step

In the second step, under the condition that σ_{02}, m_2, σ_{03} and m_3 are already known, we can estimate the remaining two unknown parameters (σ_{04}, m_4) from the data of $\phi = 90°$. Since the maximum likelihood equations in this case take very complicated forms, we directly maximize the likelihood function using the simplex method.

When the mean interval of grinding grooves, δ, is unknown, we may use a new parameter $\sigma_{04'}$ instead of σ_{04} as

$$\sigma_{04'} = \sigma_{04}\delta^{1/m_4} \quad (17)$$

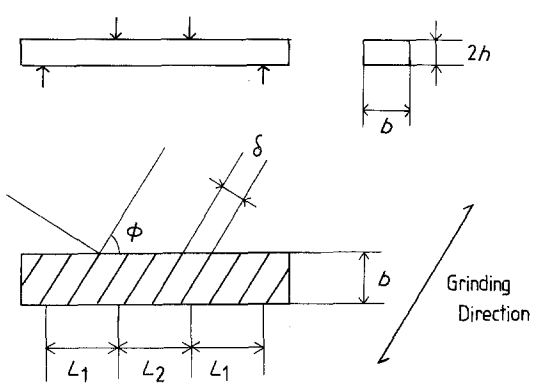

Figure 3 Dimensions and coordinate systems of the beam specimen with ground surface in four-point bending test.

TABLE I Properties of alumina specimen (SSA-S(A))

Mean grain diameter (μm)	2.0–4.0
Maximum grain diameter (μm)	10–12
Bulk density (g cm^{-3})	3.83
Purity (%)	99.56
Sintered temperature (° C)	1610–1630

3. Experimental procedure

The specimens used in this investigation were commercial sintered polycrystalline alumina SSA-S(A) manufactured by Nihon Kagaku Tougyou Co. Ltd. Each specimen was pressed and sintered individually; the final specimen size was 3 mm × 10 mm × 50 mm. The properties of SSA-S(A) are given in Table I.

The grinding processes were performed on the surface of each specimen using a resin-bonded diamond wheel (200 mm diameter) at a wheel speed of 1800 m min^{-1} and a table speed of 8 to 10 m min^{-1}. Five different diamond wheels were chosen for this study. Their grit sizes and downfeeds are shown in Table II. The downfeeds (removal rates of down grinding) were approximately one-tenth of the maximum abrasive diameters.

First, each specimen mounted on a steel plate was ground with nos 400 and 1000 diamond wheels in order to reduce the effect of pre-existing surface cracks of the materials, and then final grinding was performed. Five grinding directions, ϕ = 0°, 22.5°, 45°, 67.5° and 90° were chosen. Final grindings were carried out using nos 170, 270, 400, 600 and 1000 diamond wheels to investigate the effect of surface finishing on the bending strength. After grinding, specimens were dried in an oven at 200° C for 2 h to remove them from a steel plate, and their surfaces were cleaned by acetone.

The edges of the specimens were manually chamfered using a diamond grinding disc (mean grit sizes 6 μm) to decrease the probability of failure initiating from the edges, and edges were bevelled approximately by 2 μm.

Bending strength was measured by the four-point bending test (upper span 13.3 mm, lower span 40 mm) at room temperature with the ground surface of the specimen in tension as illustrated in Fig. 3. The cross head speed was 0.2 mm min^{-1} and the fracture strength was measured using a 500 kg load cell.

TABLE II Abrasive diameter and downfeeds

Wheel no.	Abrasive diameter (μm)	Downfeed (μm)
170	85–90	8.0
270	50–55	6.0
400	40–45	4.0
600	25–30	2.0
1000	10–15	2.0

Fracture origins were located by fluorescent dye penetration. Specimens fractured by bending test were immersed in fluorescent dye, and macroscopic surface cracks could then easily be observed under ultraviolet light because of illumination of the fluorescent dye which had penetrated into the cracks [32]. However, it is obvious that it is impossible to distinguish the pre-existing surface crack and scratch surface crack by this method. This difficulty is not, however, an obstacle for estimating the Weibull parameters as stated in Section 3.

4. Results and discussion

4.1. The effect of surface finishing on the bending strength

Bending strengths of alumina obtained in the experiment are shown in Figs. 4a and b as a function of the abrasive diameter (ϕ = 0° and ϕ = 90°). It can be seen from the figures that the bending strength of ϕ = 90° decreases with increasing abrasive diameter, while that of ϕ = 0° remains almost constant. Thus the effect of surface finishing on the bending strength perpendicular to the grinding direction (ϕ = 90°) is more severe than that parallel to the grinding direction (ϕ = 0°). These experimental results suggest that the bending strengths of alumina with a ground surface are not influenced by radial cracks perpendicular to the grinding direction but by median cracks parallel to the grinding direction. As the fracture origins of the specimens ground by no. 170 diamond wheel are all located by the fluorescent dye penetration method, a triple-modal Weibull distribution function (Equation 12) is applied to these data and the Weibull parameters are estimated using failure diagnostic data and fracture strengths. For reference, the bi-modal Weibull distribution function involving the effects of both pre-existing surface and scratch cracks, but

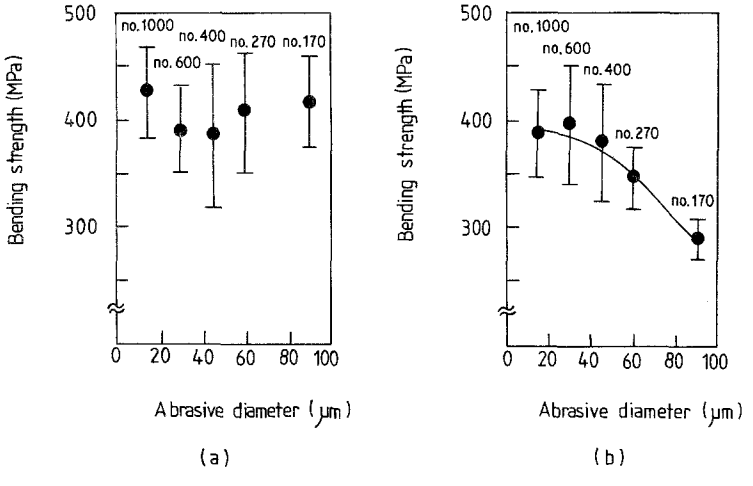

Figure 4 Effects of surface finishing on four-point bending strength: (a) grinding direction ϕ = 0° (parallel to the beam axis); (b) grinding direction ϕ = 90° (perpendicular to the beam axis).

TABLE III The estimated Weibull parameters and mean strength

Grinding angle			Wheel no.				
			170	270	400	600	1000
$\phi = 0°$	Mean strength (MPa)		416	409	387	389	424
	Standard deviation (MPa)		40.0	52.6	61.2	35.4	46.5
	Pre-existing surface:	m_2	11.0	9.31	7.47	13.4	11.0
		σ_{02}	711	728	807	573	684
	Pre-existing edge:	m_3	18.4				
		σ_{03}	523				
$\phi = 90°$	Mean strength (MPa)		283	351	381	398	386
	Standard deviation (MPa)		22.6	34.4	56.1	48.7	49.2
	Scratch:	m_4	13.3	13.3	15.4		
		$\sigma_{04'}$	413	546	658		

neglecting that of edge cracks, are applied to the specimens ground with other diamond wheels. Mean strengths, standard deviations and estimated Weibull parameters are summarized in Table III.

We now consider the relation between the maximum abrasive diameter and the equivalent critical flaw depth (C_f) which is defined by

$$C_f = \beta^2 K_{Ic}^2/\pi\sigma_f^2$$

where β is a constant (≈ 1.1215), σ_f is the fracture stress, K_{Ic} is the fracture toughness. The results are shown in Fig. 5. We see from this figure that the value of critical flaw depth (C_f) is constant in the region where the abrasive diameter (D_a) is smaller than 40 μm. This means that in this region the pre-existing cracks are dominant and the scratch cracks hardly influence the bending strength. If D_a is larger than 40 μm, the critical flaw depth (C_f) increases linearly with abrasive diameter, because the machining-induced cracks are the main failure origin in most cases. In this region, the general relation between the bending strength and the surface finishing may be expressed as

$$\sigma_f = K_{Ic}/\beta(\pi C)^{1/2} = \zeta D_a^{-1/2}$$
$$(D_a > 40\,\mu\text{m}, \zeta = \text{constant})$$

The knee point in Fig. 5 is highly important in material design because this point is the reflection of the micro-structure of the materials.

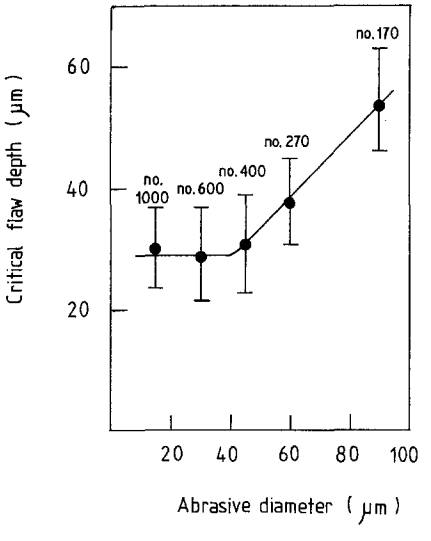

Figure 5 Estimated critical flaw depth as a function of surface finishing. $\phi = 90°$.

4.2. The effect of grinding direction on the bending strength

The relations between grinding directions and bending strengths of alumina ground with no. 170 diamond wheel are shown in Fig. 6. It is evident from the figure that median cracks parallel to the grinding direction strongly influence the bending strengths of the materials. The curve in Fig. 6 is the theoretical mean value obtained from Equation 12. The theoretical curve coincides well with the experimental results.

The probability density functions are calculated in order to discuss competing risks (pre-existing surface, pre-existing edge and scratch cracks). The probability density function (p.d.f.) of each risk is given by

$$\text{surface: } f_2(\sigma) = (\partial B_2/\partial\sigma)\exp(-B_2)$$
$$\text{edge: } f_3(\sigma) = (\partial B_3/\partial\sigma)\exp(-B_3)$$
$$\text{scratch: } f_4(\sigma) = (\partial B_4/\partial\sigma)\exp(-B_4)$$
$$\text{total: } f_t(\sigma) = (\partial B_2/\partial\sigma + \partial B_3/\partial\sigma + \partial B_4/\partial\sigma) \times \exp(-B_2 - B_3 - B_4)$$

The calculated results which were obtained using the equations described above are shown in Fig. 7 with varying the grinding direction. In the region $\phi \geqslant 67.5°$, the p.d.f. of "total" coincides with that of "scratch". This fact means that the scratch cracks are dominant in this region. At $\phi = 45°$ we see that three kinds of risks are competing. On the other hand, in the region $\phi \leqslant 22.5°$, the scratch cracks no longer contribute to the total p.d.f.

5. Conclusion

A new distribution function for fracture strength based on multi-modal Weibull distribution function has been suggested in order to estimate the fracture behaviour of brittle materials with ground surfaces. The bending tests of alumina ceramics ground by diamond wheels have been carried out and the following results were obtained.

1. The fracture origins of alumina specimens with ground surfaces are controlled by the competing relation between the pre-existing cracks and the machining-induced scratch cracks.

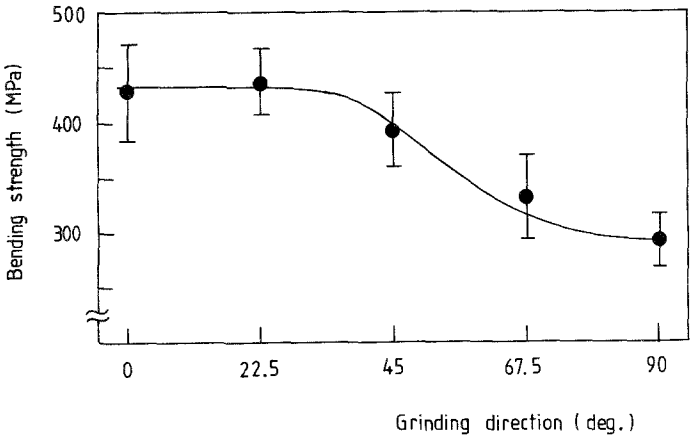

Figure 6 Effects of the grinding direction on four-point bending strength and expected value calculated from Equation 12.

2. The distribution functions formulated in this work can explain the anisotropy of the bending strengths of alumina specimens with a ground surface fairly well.

3. The bending strengths of alumina used in this experiment are proportional to $-1/2$ powers of the abrasive diameter in the region larger than 40 μm.

References

1. A. G. EVANS, National Bureau of Standards Special Publication, Washington, D.C., 562 (1979) p.1.
2. H. P. KIRCHNER, R. M. GRUVER and D. M. RICHARD, *ibid.* 562 (1979) p. 23.
3. R. W. RICE and J. J. MECHOLSKY Jr, *ibid.* 562, p. 351.
4. R. W. RICE, *ibid*, 562, p. 429.
5. H. P. KIRCHNER and E. D. ISAACSON, *J. Amer. Ceram. Soc.* **65** (1982) 55.
6. D. W. RICHERSON, "Modern ceramic engineering" (Marcel Dekker, New York and Basel, 1982) pp. 260–73.
7. A. BROESE VAN GROENOU, N. MAAN and J. B. D. VELDKAMP, National Bureau of Standards Special Publication, Washington, D.C., 562 (1979) p. 43.
8. S. MALKIN and M. HEURTA, *ibid*, **562** (1978) p. 93.
9. T. E. EASLER, T. A. COUNTERMINE, R. E. TRESSLER and R. C. BRADT, *ibid*, 562 (1979) p. 455.
10. C. Cm. WU and K. R. McKINNEY, *ibid*, 562 (1979) p. 477.
11. H. W. HAWMAN, P. H. COHEN, J. C. CONWAY and R. N. PANGBORN, *J. Mater. Sci.* **20** (1985) 482.
12. J. J. MECHOLSKY Jr, S. W. FREIMAN and R. W. RICE, *J. Amer. Ceram. Soc.* **60** (1977) 114.
13. C. A. ANDERSSON and R. J. BRATTON, National Bureau of Standards Special Publication, Washington, D.C., 562 (1979) p. 463.
14. R. E. TRESSLER, R. A. LANGENSIEPEN and R. C. BRADT, *J. Amer. Ceram. Soc.* **57** (1974) 226.
15. D. C. CRANMER, R. E. TRESSLER and R. C. BRADT, *ibid.* **60** (1977) 230.
16. M. HAKULINEN, *J. Mater. Sci.* **20** (1985) 1049.
17. J. J. PETROVIC and M. G. MENDIRATTA, *J. Amer. Ceram. Soc.* **59** (1976) 163.
18. S. W. FREIMAN, A. C. GONZALEZ and J. J. MECHOLSKY *ibid.* **62** (1979) 206.
19. D. B. MARSHALL, *ibid.* **67** (1984) 110.
20. W. A. WEIBULL, *Ingenioersvetenskapsakad. Handl.* No. 151 (1939) 45pp.
21. S. B. BATDORF and J. G. CROSE, *Trans. ASME E* **41** (1974) 459.
22. S. B. BATDORF, in "Fracture mechanics of ceramics", Vol. 3, edited by R. C. Bradt, D. P. H. Hasselman and F. F. Lange (Plenum, New York, 1978) p.1.
23. A. G. EVANS, *ibid.*, Vol. 3, p. 31.
24. A. G. EVANS, *J. Amer. Ceram. Soc.* **61** (1979) 302.

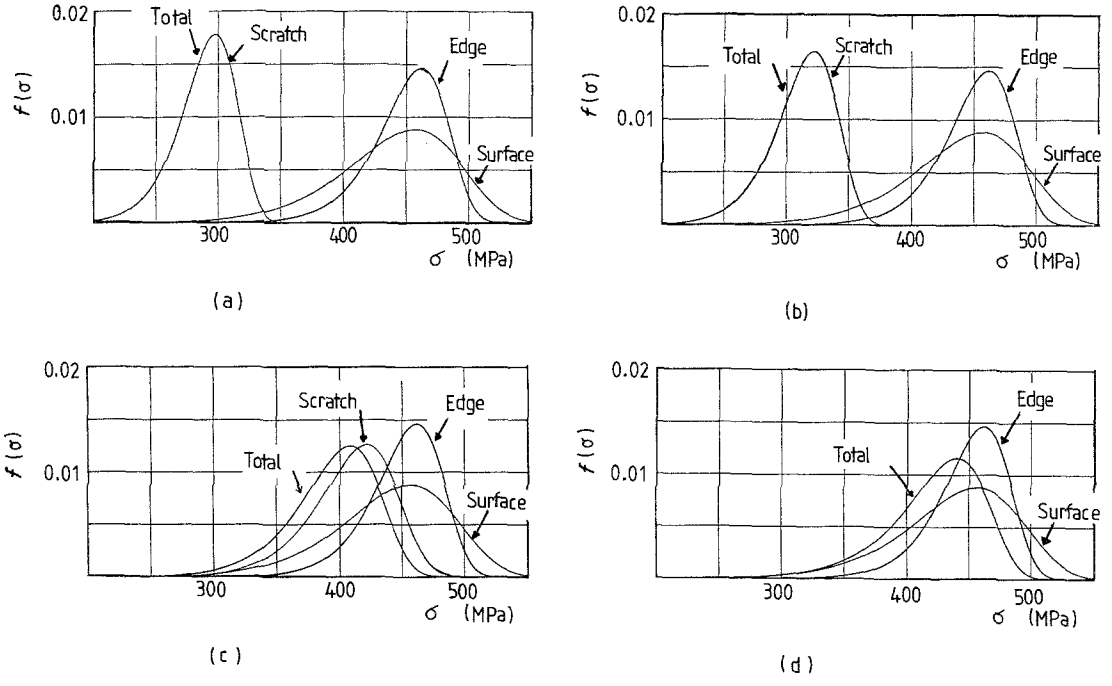

Figure 7 Calculated probability density functions of individual risk of rupture with varying grinding direction ϕ: (a) $\phi = 90°$; (b) $\phi = 67.5°$; (c) $\phi = 45°$; (d) $\phi = 0°$, 22.5°.

25. Y. MATSUO, *Trans. JSME. A* **46** (1980) 605.
26. Y. MATSUO, *Eng. Fract. Mech.* **14** (1981) 527.
27. V. V. BOLOTIN, "Statistical Methods in structural Mechanics' (Holden-Day, San Francisco, 1969).
28. C. A. JOHNSON, in "Fracture mechanics of ceramics," Vol. 5, edited by R. C. Bradt, D. P. H. Hasselman and F. R. Lange (Plenum, New York, 1978) p. 365.
29. Y. MATSUO and H. MURATA, *J. Soc. Mater. Sci. Japan* **33** (1984) 1545.
30. M. R. SAMPFORD, *Biometrics* **8** (1952) 307.
31. D. SONDERMAN, *J. Mater. Sci.* **20** (1985) 207.
32. Y. MATSUO, T. OGASAWARA, T. KITABAYASHI, E. YASUDA and S. KIMURA, *Yogyo-Kyoukai-shi* **93** (1985) 668.

Received 9 June
and accepted 18 August 1986